Observation of variations in cosmic ray single count rates during thunderstorms and implications for large-scale electric field changes

R. U. Abbasi et al.

Phys. Rev. D **105**, 062002 — Published 18 March 2022

DOI: 10.1103/PhysRevD.105.062002

Observation of Variations in Cosmic Ray Single Count Rates During Thunderstorms and Implications for Large-Scale Electric Field Changes

R.U. Abbasi,[1,*] T. Abu-Zayyad,[1,2] M. Allen,[2] Y. Arai,[3] R. Arimura,[3] E. Barcikowski,[2] J.W. Belz,[2] D.R. Bergman,[2] S.A. Blake,[2] I. Buckland,[2] R. Cady,[2] B.G. Cheon,[4] J. Chiba,[5] M. Chikawa,[6] T. Fujii,[7] K. Fujisue,[6] K. Fujita,[3] R. Fujiwara,[3] M. Fukushima,[6] R. Fukushima,[3] G. Furlich,[2] N. Globus,[8,†] R. Gonzalez,[2] W. Hanlon,[2] M. Hayashi,[9] N. Hayashida,[10] K. Hibino,[10] R. Higuchi,[6] K. Honda,[11] N. Husseini,[12] D. Ikeda,[10] T. Inadomi,[13] N. Inoue,[14] T. Ishii,[11] H. Ito,[8] D. Ivanov,[2] H. Iwakura,[13] A. Iwasaki,[3] H.M. Jeong,[15] S. Jeong,[15] H. Johnson,[1] C.C.H. Jui,[2] K. Kadota,[16] F. Kakimoto,[10] O. Kalashev,[17] K. Kasahara,[18] S. Kasami,[19] H. Kawai,[20] S. Kawakami,[3] S. Kawana,[14] K. Kawata,[6] I. Kharuk,[17] E. Kido,[8] H.B. Kim,[4] J.H. Kim,[2] J.H. Kim,[2] M.H. Kim,[15] S.W. Kim,[15] Y. Kimura,[3] S. Kishigami,[3] Y. Kubota,[13] S. Kurisu,[13] V. Kuzmin,[17,‡] M. Kuznetsov,[21,17] Y.J. Kwon,[22] K.H. Lee,[15] R. LeVon,[2] B. Lubsandorzhiev,[17] J.P. Lundquist,[23,2] K. Machida,[11] H. Matsumiya,[3] T. Matsuyama,[3] J.N. Matthews,[2] R. Mayta,[3] J. Mazich,[1] M. Minamino,[3] K. Mukai,[11] I. Myers,[2] P. Myers,[1] S. Nagataki,[8] K. Nakai,[3] R. Nakamura,[13] T. Nakamura,[24] T. Nakamura,[13] Y. Nakamura,[13] A. Nakazawa,[13] E. Nishio,[19] T. Nonaka,[6] K. O'Brien,[1] H. Oda,[3] S. Ogio,[25,3] M. Ohnishi,[6] H. Ohoka,[6] Y. Oku,[19] T. Okuda,[26] Y. Omura,[3] M. Ono,[8] R. Onogi,[3] A. Oshima,[27] S. Ozawa,[28] I.H. Park,[15] M. Potts,[2] M.S. Pshirkov,[17,29] J. Remington,[2] D.C. Rodriguez,[2] G.I. Rubtsov,[17] D. Ryu,[30] H. Sagawa,[6] R. Sahara,[3] Y. Saito,[13] N. Sakaki,[6] T. Sako,[6] N. Sakurai,[3] K. Sano,[13] K. Sato,[3] T. Seki,[13] K. Sekino,[6] P.D. Shah,[2] Y. Shibasaki,[13] F. Shibata,[11] N. Shibata,[19] T. Shibata,[6] H. Shimodaira,[6] B.K. Shin,[30] H.S. Shin,[6] D. Shinto,[19] J.D. Smith,[2] P. Sokolsky,[2] N. Sone,[13] B.T. Stokes,[2] T.A. Stroman,[2] Y. Takagi,[3] Y. Takahashi,[3] M. Takamura,[5] M. Takeda,[6] R. Takeishi,[6] A. Taketa,[31] M. Takita,[6] Y. Tameda,[19] H. Tanaka,[3] K. Tanaka,[32] M. Tanaka,[33] Y. Tanoue,[3] S.B. Thomas,[2] G.B. Thomson,[2] P. Tinyakov,[21,17] I. Tkachev,[17] H. Tokuno,[34] T. Tomida,[13] S. Troitsky,[17] R. Tsuda,[3] Y. Tsunesada,[25,3] Y. Uchihori,[35] S. Udo,[10] T. Uehama,[13] F. Urban,[36] T. Wong,[2] M. Yamamoto,[13] K. Yamazaki,[27] J. Yang,[37] K. Yashiro,[5] F. Yoshida,[19] Y. Yoshioka,[13] Y. Zhezher,[6,17] and Z. Zundel[2]

[1] *Department of Physics, Loyola University Chicago, Chicago, Illinois, USA*
[2] *High Energy Astrophysics Institute and Department of Physics and Astronomy, University of Utah, Salt Lake City, Utah, USA*
[3] *Graduate School of Science, Osaka City University, Osaka, Osaka, Japan*
[4] *Department of Physics and The Research Institute of Natural Science, Hanyang University, Seongdong-gu, Seoul, Korea*
[5] *Department of Physics, Tokyo University of Science, Noda, Chiba, Japan*
[6] *Institute for Cosmic Ray Research, University of Tokyo, Kashiwa, Chiba, Japan*
[7] *The Hakubi Center for Advanced Research and Graduate School of Science, Kyoto University, Kitashirakawa-Oiwakecho, Sakyo-ku, Kyoto, Japan*
[8] *Astrophysical Big Bang Laboratory, RIKEN, Wako, Saitama, Japan*
[9] *Information Engineering Graduate School of Science and Technology, Shinshu University, Nagano, Nagano, Japan*
[10] *Faculty of Engineering, Kanagawa University, Yokohama, Kanagawa, Japan*
[11] *Interdisciplinary Graduate School of Medicine and Engineering, University of Yamanashi, Kofu, Yamanashi, Japan*
[12] *Illinois Mathematics and Science Academy, Aurora, Illinois, USA*
[13] *Academic Assembly School of Science and Technology Institute of Engineering, Shinshu University, Nagano, Nagano, Japan*
[14] *The Graduate School of Science and Engineering, Saitama University, Saitama, Saitama, Japan*
[15] *Department of Physics, SungKyunKwan University, Jang-an-gu, Suwon, Korea*
[16] *Department of Physics, Tokyo City University, Setagaya-ku, Tokyo, Japan*
[17] *Institute for Nuclear Research of the Russian Academy of Sciences, Moscow, Russia*
[18] *Faculty of Systems Engineering and Science, Shibaura Institute of Technology, Minato-ku, Tokyo, Japan*
[19] *Department of Engineering Science, Faculty of Engineering, Osaka Electro-Communication University, Neyagawa-shi, Osaka, Japan*
[20] *Department of Physics, Chiba University, Chiba, Chiba, Japan*
[21] *Service de Physique Thorique, Universit Libre de Bruxelles, Brussels, Belgium*
[22] *Department of Physics, Yonsei University, Seodaemun-gu, Seoul, Korea*
[23] *Center for Astrophysics and Cosmology, University of Nova Gorica, Nova Gorica, Slovenia*
[24] *Faculty of Science, Kochi University, Kochi, Kochi, Japan*
[25] *Nambu Yoichiro Institute of Theoretical and Experimental Physics, Osaka City University, Osaka, Osaka, Japan*
[26] *Department of Physical Sciences, Ritsumeikan University, Kusatsu, Shiga, Japan*
[27] *College of Engineering, Chubu University, Kasugai, Aichi, Japan*
[28] *Quantum ICT Advanced Development Center, National Institute for Information and Communications Technology, Koganei, Tokyo, Japan*
[29] *Sternberg Astronomical Institute, Moscow M.V. Lomonosov State University, Moscow, Russia*
[30] *Department of Physics, School of Natural Sciences, Ulsan National Institute of Science and Technology, UNIST-gil, Ulsan, Korea*

[31] *Earthquake Research Institute, University of Tokyo, Bunkyo-ku, Tokyo, Japan*
[32] *Graduate School of Information Sciences, Hiroshima City University, Hiroshima, Hiroshima, Japan*
[33] *Institute of Particle and Nuclear Studies, KEK, Tsukuba, Ibaraki, Japan*
[34] *Graduate School of Science and Engineering, Tokyo Institute of Technology, Meguro, Tokyo, Japan*
[35] *Department of Research Planning and Promotion, Quantum Medical Science Directorate, National Institutes for Quantum and Radiological Science and Technology, Chiba, Chiba, Japan*
[36] *CEICO, Institute of Physics, Czech Academy of Sciences, Prague, Czech Republic*
[37] *Department of Physics and Institute for the Early Universe, Ewha Womans University, Seodaaemun-gu, Seoul, Korea*

We present the first observation by the Telescope Array Surface Detector (TASD) of the effect of thunderstorms on the development of cosmic ray single count rate intensity over a 700 km^2 area. Observations of variations in the secondary low-energy cosmic ray counting rate, using the TASD, allow us to study the electric field inside thunderstorms, on a large scale, as it progresses on top of the 700 km^2 detector, without dealing with the limitation of narrow exposure in time and space using balloons and aircraft detectors. In this work, variations in the cosmic ray intensity (single count rate) using the TASD, were studied and found to be on average at the $\sim (0.5-1)\%$ and up to 2% level. These observations were found to be both in excess and in deficit. They were also found to be correlated with lightning in addition to thunderstorms. These variations lasted for tens of minutes; their footprint on the ground ranged from 6 to 24 km in diameter and moved in the same direction as the thunderstorm. With the use of simple electric field models inside the cloud and between cloud to ground, the observed variations in the cosmic ray single count rate were recreated using CORSIKA simulations. Depending on the electric field model used and the direction of the electric field in that model, the electric field magnitude that reproduces the observed low-energy cosmic ray single count rate variations was found to be approximately between 0.2-0.4 GV. This in turn allows us to get a reasonable insight on the electric field and its effect on cosmic ray air showers inside thunderstorms.

I. INTRODUCTION

Understanding lightning initiation is one of the most important questions in atmospheric physics. The heart of the problem of understanding lightning initiation is that, with decades of electric fields measurements, the observed values of detected electric field are not sufficient to create a leader or a stroke propagating on a kilometer(s) scale [1, 2]. This could mean that either our understanding of how lightning is initiated or electric field measurements in thunderstorms are inaccurate.

Traditionally, balloons and planes are used to make such measurements. However, there are limitations to obtaining such observations. At first, sending planes, balloons, and launching rockets inside thunderstorms can be quite difficult and dangerous. Moreover, thunderstorms can span up to square kilometers in size, while the electric field measured by airplanes and balloons spans a small region in comparison. To be in the right location at the right time where the electric field and the potential difference are of a high value can be of low probability. Most importantly, the instrument sent inside a thunderstorm might be responsible for discharging the thunderstorm itself before the electric field has the chance to build up.

When cosmic ray particles interact in the atmosphere, they produce a shower of secondary particles. During thunderstorms, these showers of secondary particles would accelerate or decelerate, depending on their charge and magnitude of the electric field they are propagating through. In principle, studying the effect of the electric field on these secondary particles would allow us to measure and model the electric field in their path indirectly.

The effect of thunderstorms on extensive air showers is a hot topic that has been reported on by multiple experiments starting with the Baksan group in 1985 [3]. They argued that the effect of the observed cosmic ray variations in the hard and soft components of the shower are due to the electric field in the atmosphere. Several studies and observations have followed EAS-TOP [4], Mount Norikura [9], GROWTH [8], Tibet AS [5], ARGO-YBJ [6], and SEVAN [7], reporting on the cosmic ray secondary showers (electrons, gamma rays, muons, and neutrons) variation in correlation with thunderstorms. Most recently, a potential difference of greater than 1 GV inside a cloud (predicted by C.T.R. Wilson 90 years ago [10]) was indirectly measured in a storm by the Grapes-3 Muon Telescope scientists [11]. Such potential difference is almost an order of magnitude larger than the previously reported maximum potential in balloon sounding (0.13 GV) [11, 12].

In this work, we will present the effect of the electric field in thunderstorms on the extensive air showers as observed by the Telescope Array Surface Detector (TASD) single count rate. We will report on the observations in the variation of secondary cosmic-ray single count rate (See the trigger level discussion in Section II) . The variations are slow, several kilometers square in area, and moves together with the thunderstorm on top of the 700

* rabbasi@luc.edu
† Presently at: University of Californa - Santa Cruz and Flatiron Institute, Simons Foundation
‡ Deceased

km^2 detector. In comparison to detectors that are spread over less than km^2 in area (i.e. [8]), it is unclear if the gamma ray emission ceases when the thunderstorm disappears, or when the gamma ray source moves away from the detectors observing the rate variation, as the thunderclouds moves. We will attempt, to report on this question, for the first time, using a large area coverage of 700 km^2. Moreover, we will attempt to interpret this variation, by simulating the effect of the electric field in thunderstorms using multiple simple models. The corresponding increase and decrease of the rate variation in correlation with these models is reproduced and discussed.

II. THE TELESCOPE ARRAY DETECTOR

The Telescope Array (TA) detector is located in the southwestern desert of the State of Utah about 1400 m above sea level. Currently it is the largest Ultra High Energy Cosmic Ray (UHECR) experiment in the Northern Hemisphere. The TA detector is comprised of Surface Detectors (SDs) surrounded by three Fluorescence Detectors (FDs). The main goal of the TA detector is to explore the origin of UHECRs using their energy, composition, and arrival direction. The FD, which operates on clear moonless nights (approximately 10% duty cycle) provides a measurement of the longitudinal profile of the Extensive Air Shower (EAS) induced by the primary UHECR, as well as a calorimetric estimate of the EAS energy. The SD part of the detector, with approximately 100% duty cycle, provides shower footprint information including core location, lateral density profile, and timing, which are used to reconstruct shower geometry and energy.

The Surface Detector utilizes plastic scintillators to observe the EAS footprint produced by primary cosmic ray interactions in the atmosphere. Plastic scintillators are sensitive to all charged particles. The Surface Detector array (SD) part of the TA experiment, is composed of 507 scintillator detectors on a 1.2 km square grid covering 700 km^2 in area shown in Figure 1. Each surface detector houses two layers of plastic scintillator. Each layer of scintillator has an area of 3 m^2 and a thickness of 1.2 cm. Each plastic scintillator slab has grooves that has 104 WaveLength-Shifting (WLS) fibers running through them collecting light into PMTs they are bundled and connected to. These scintillator layers are separated by a 1 mm stainless-steal plate. The scintillator layers and stainless-steal plate are housed in light tight, 1.5 mm thick box made of grounded stainless steel (top cover is 1.5 mm thick, with a 1.2 mm thick bottom) under an additional 1.2 mm iron roof providing protection from extreme temperature variations [13].

There are a total of three trigger data levels. Level-0, Level-1, and Level-2. Charged particles triggering a single counter (both the upper and the lower scintillators) with an energy above approximately 0.3 Minimum Ionizing Particle (MIP) ($\sim$ 0.75 MeV) are stored in a memory buffer on CPU board as Level-0 trigger data (trigger rate is approximately 750 Hz). Charged particles triggering the detector with an energy above approximately 3 MIPs are stored as a level-1 trigger event (trigger rate is approximately 30 Hz).When three adjacent detectors trigger with an energy above 3 MIPs within 8 μseconds the data is saved as Level-2 trigger (trigger rate is approximately 0.01 Hz). Level-2 trigger is the one used to study UHECRs and Level-0's main goal is to monitor the health of the detector. In this work we are using the

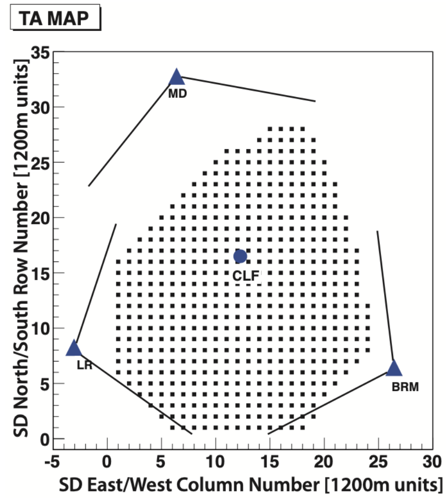

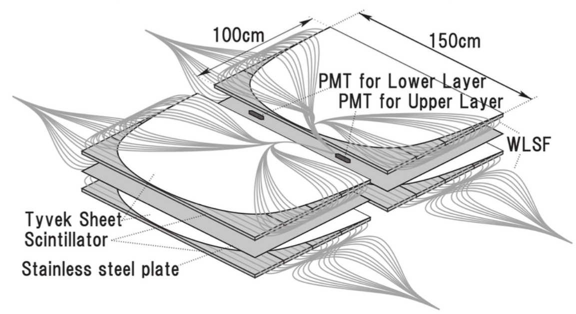

FIG. 1. *top:* The Telescope Array, consisting of 507 scintillator Surface Detectors (SDs) on a 1.2 km grid over a 700 km^2 area. The SD scintillators are enclosed by three fluorescence detectors shown in filled triangles together with their field of view in solid lines. The northernmost fluorescence detector is called Middle Drum while the southern fluorescence detectors are referred to as Black Rock Mesa and Long Ridge. The filled circle in the middle equally spaced from the three fluorescence detectors is the Central Laser Facility used for atmospheric monitoring and detector calibration. *Bottom:* Schematic sketch of the upper and lower 1.2 cm thick plastic scintillator layers inside the scintillator box, the 1 mm stainless steel plate, the 104 wavelength-shifting (WLS) fibers and the photomultiplier tubes (PMTs). These items are enclosed in a stainless steel box, 1.5 mm thick on top and 1.2 mm thick on the bottom. [13].

rate of the detected particles every 10 minutes recorded by Level-0 trigger dominated by the single particles with primary energy ranging between $\sim 2 \times 10^{10} - 10^{13}$ eV.

The TASD is designed to detect the charged components (primarily electrons, positrons, and muons) of the Extensive Air Shower (EAS). The response of the detector has been discussed in detail in [13, 14]. Mostly muons and electrons are detected above approximately 30 MeV. Below this, the total energy deposited by muons and electrons falls off rapidly; below 1 MeV there is no detectable energy deposit as the electrons fail to penetrate a significant depth into the scintillator [14].

III. OBSERVATIONS

The Telescope Array detector has been in operation since 2008. Thunderstorms continuously pass on top of the Telescope Array detector. In this work, we searched for possible variation in the cosmic ray single count rate using Level-0 trigger in correlation with National Lightning Detection Network (NLDN) activity. There are typically about 750 NLDN recorded flashes (intra-cloud and cloud-to-ground) per year over the 700 km^2 TASD array. Due to the large number of flashes only days with thunderstorms including a high recorded peak currents (>90 kA) are incorporated in the current search. For the level-0 trigger data collected between 2008-2011, several thunderstorms were observed to produce a variation in the cosmic ray single count rate, the variations were observed during lightning events and in correlation with thunderstorms in the absence of lightning.

As an example, we chose an event observed on September 27 2014 shown in Figure 2. In Figure 2, each frame lasts for ten minutes in duration. The time of the start of each frame is denoted on each frame in UTC. The color scale represents the change of the rate in Level-0 trigger of the current frame N_c from the ten minute frame right before it N_p divided by N_p ($\frac{N_c - N_p}{N_p}$) or ($\Delta N/N$). Lightning events reported by the NLDN locations are also added in each of the frames in Figure 2 and in the supporting information (SI1). Intra-Cloud in black and Cloud-to-Ground in grey. It is worth noting that three Terrestrial Gamma-ray Flashes (TGFs) were reported in [14] on this day. One of these TGFs was reported at 07:54:35 (during the first frame in Figure 2).

One can see a movement of a deficit in the intensity variation $\Delta N/N$ for 30 minutes (from 7:50-8:20 in UTC) in correlation with lightning activity. In addition, an excess was also found for 30 minutes (from 19:00-19:30 in UTC) in the intensity variation $\Delta N/N$ during which no lightning activity was reported by NLDN (supporting information, (SI1)). These variations are both seen in correlation with lightning (using NLDN) and thunderstorms (using radar images) in addition or in the absence of lightning (see supporting information videos (SI4, SI5)). The variations correlation with pressure is not available at the current time resolution at the ground level. However, the variations were found to be not correlated with temperature changes at the ground level as shown in Figure 3 and in the supporting information in (SI2). The size of the variation ranged for this thunderstorm from 6 to 24 km in diameter on the ground. The variations were observed in excess and deficit modes over 10 minutes in durations mostly between $\pm$(0.5-1)% and can reach up to 2% in magnitude.

IV. CORSIKA SIMULATIONS

The main goal of this simulation work is to quantify the electric field inside thunderstorms resulting in the observed variations in the single count rate by the TASD detector. To do this we need to learn the conversion of the observed ($\Delta N/N$) into the equivalent potential model. This is done by inserting the atmospheric electric field model into the CORSIKA simulations. Here the CORSIKA package used in this simulation work is 7.6900 [15], where cosmic rays and their extensive air shower particles propagate through the atmosphere and through the implemented electric field model. Both the electromagnetic and the muonic components of the showers are traced through the atmosphere and the implemented electric field model until they reach the detector observational level ($\sim$ 1400 m).

As a start, two electric field models are used. Note that both models chosen are the simplest electric field models that allow us to reproduce the main observed ($\Delta N/N$) values. Both models use a uniform electric field layer. The first model uses a uniform electric field 2 km inside the thundercloud that is located 2 km above ground level. The second model uses a uniform electric field between the thundercloud base and the ground. Both models are illustrated in the Supporting Information (SI3) in the supporting information. In this second model the thundercloud base is 2 km in height from the detector. While thunderstorms structures are known to be complex, both the thundercloud length and height from the ground used in this work are reasonably representative of thunderstorms at the Southwestern desert of Utah [14].

Primary cosmic ray particles composed of protons were generated between 20 GeV -10 TeV. SIBYLL2.3c [16] is used for the high energy interaction (> 80 GeV). While, GHEISHA [17], URQMD [18], and FLUKA [19] are used for the low energy model (< 80 GeV). The zenith and azimuth range from $0° \leq \theta \leq 60°$ and $0° \leq \phi \leq 360°$. The energy threshold of secondary particles were traced until they reach the following energies: 0.05 GeV for hadrons, 0.5 GeV for muons, 0.001 GeV for electrons and 0.001 GeV for gammas.

The simulation was curried out first with no electric field for background. Second, by applying an electric field value that ranges between -2000 to +2000 V/cm (-200 to +200 kV/m). Figure 4 shows the distribution of the electromagnetic (γ,e$^{\pm}$) and muonic shower components ($\mu^{\pm}$) on the ground at 1400 m propagated through the

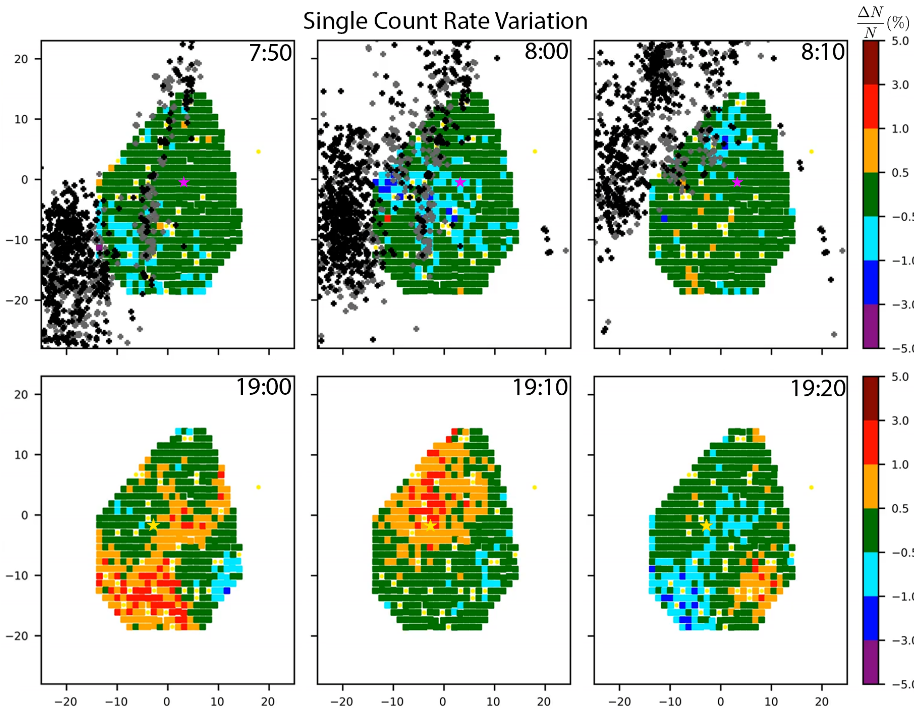

FIG. 2. Time evolution of the intensity variation of the single count rate change ($\frac{N_c - N_p}{N_p}$)% or $(\Delta N/N)$% on the 09/27/2014 thunderstorm. Each time frame is ten minutes in duration. The starting time in UTC is denoted on each frame. The black and grey crosses marks are the Intra-Cloud and Cloud-to-Ground lightning sources detected by the NLDN for each frame. The two yellow and pink stars point at the two detectors (1516 (denoted in pink) and 1015 (denoted in yellow)) plotted in Figure 3.

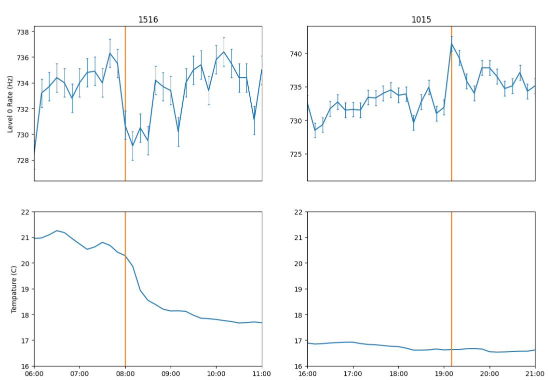

FIG. 3. Rate variation vs. time and temperature variation vs. time for two detectors numbered (1516 and 1015). Here 1516 shows a deficit in the rate variation (-0.8%) and 1015 shows an excess in the rate variation (+1.3%).

atmosphere with electric field at $\pm$ 2000 V/cm and without an electric field from cloud to ground. The air shower particles (γ,e$^{\pm}$, and $\mu^{\pm}$) are then propagated through the SD detector using an energy dependent response function derived from GEANT4 simulation of the surface detector [14] and following the same trigger condition as the level-0 trigger. The dependence of $(\Delta N/N)$ on the potential inside the thunderstorms is shown in Figure 5 using both thunderstorm electric field models described in this section. Note that, the direction of the electric field follows CORSIKA's definition, where positive electric field direction is pointing upwards.

V. DISCUSSION

The simulation results shown in Figure 5 presents $(\Delta N/N)$ vs. the potential difference (ΔV) for both investigated electric field models. The first model included a uniform electric field inside a cloud (**Intra-Cloud model** ((SI3) left)) with 2 km in thickness and two kilometers in height from the ground . This model produced both the excess and deficit observed in the variation in the cosmic ray single count rate. While we are unable to distinguish the type of triggering particle from plastic scintillators, simulations show that the deficit observed by the TASD is dominated by muons. In a negative electric field, an average deficit using the low energy models (GHEISHA, URQMD, and FLUKA), is 0.75$\pm$0.28% obtained at -0.2 GV. In a positive electric field, an average deficit of $1.3^{+1.17}_{-1.38}$% is obtained at $+0.2$ GV. As shown in Figure 2 the deficit observed by the TASD is mostly

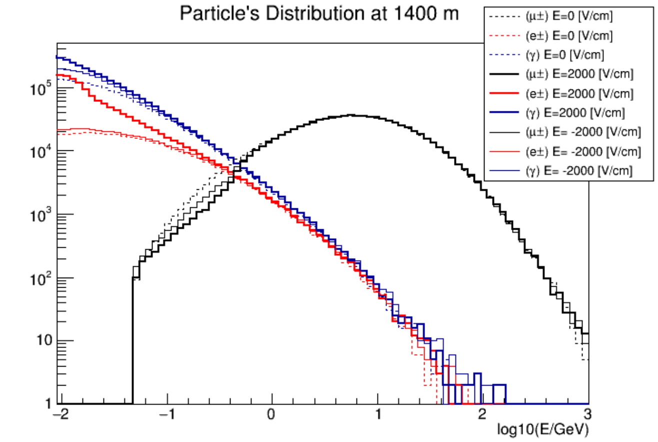

FIG. 4. The energy distributions of the muons and electromagnetic components of the EAS at 1400 m. The distribution of particles ($e^{\pm}, \mu^{\pm}, \gamma$) included in this plot are without electric field shown in dashed lines for the Cloud-to-Ground model and with electric field of + 2000 V/cm (200 kV/m or 0.4GV/2 km) effect on ($e^{\pm}, \mu^{\pm}, \gamma$) shown in thick solid lines and − 2000 V/cm effect on ($e^{\pm}, \mu^{\pm}, \gamma$) shown in thin solid lines. Detector response is not included in this distribution.

between 0.5 and 1% and can go up to 2%. This observed deficit is reproduced around ± 0.2 GV, using this model.

As the potential difference increases above 0.3 GV so does the variation in the cosmic ray single count rate turns from deficit to excess. The excess in the variation of $\Delta N/N$ strongly depends on the polarity of the electric field inside the thunderstorm in addition to the magnitude of the electric field. Simulations show that while the deficit in muons is stronger with larger potential, an excess in the total number of particles observed by the TASD is expected as the variation of the soft components of the cosmic ray air shower dominates the total number of the observed particles. It also shows that the observed excess can be obtained depending on the low energy model and polarity. The TASD observed excess is mostly between 0.5 and 1% and can go up to 2%. In a negative electric field an average excess of $1.36^{+1.18}_{-0.44}\%$ is obtained at -0.4 GV. In the positive electric field, an average excess of $0.5-2\%$ is obtained with a potential between 0.3 and 0.4 GV. For the most part, the magnitude of ΔV needed to obtain the same observed variation is larger in the negative than in the positive electric field. This asymmetry is due to the fact that the number of electrons exceeds the number of positrons in the extensive air showers. This, in addition to the fact that, there are higher numbers of electrons with lower energies than positrons. Thus the effect of positive fields (accelerating electrons) is larger than the negative field (accelerating positrons) [6].

The second model included a uniform electric field of 2 km in length from the cloud to the ground (**Cloud-to-Ground model** ((SI3) right)). This model produced only the excess in the variation in cosmic ray air single count rate (for the simulation sets produced). As in the first model, the excess in the total number of particles observed by the TASD is expected as the variation of the soft components of the cosmic ray air shower dominates the total number of observed particles. In a negative electric field, an average excess of $1.40^{+0.4}_{-0.2}\%$ can be produced by a potential difference of -0.2 GV. In a positive electric field, an excess of 0.5-2% can be produced by a potential difference of less than 0.2 GV. The excess at a potential difference of -0.4 and 0.4 GV is 20 and 40% consecutively (much larger than the maximum observed excess of 2%). Therefore, we conclude that any observed excess resulting from this model is reproduced close to ± 0.2 GV in potential.

It is important to note that, the interpretation of both models to the observations in the TASD single count variations is based on the assumption that the duration of the electric field inside the thunderstorm matches that of the duration of the ten minutes recorded observations by the Level-0 filter. However, the duration of the electric field could, in principle, be shorter than 10 minutes and therefore we can assume that our current electric field interpretation is a lower limit value to the possible electric field magnitude that is responsible for the single rate observed variations.

VI. CONCLUSION

Variation in the flux of secondary low-energy cosmic-ray counting rate in association with thunderstorms is reported in this work by the Telescope Array Surface Detector (TASD). The surface detector utilizes plastic scintillators to observe the charged components (primarily electrons, positrons, and muons) of the cosmic ray air shower. The variation in secondary low-energy cosmic-ray counting rate magnitude mostly ranges between (0.5% and 1%) and can reach up to 2%, both in excess and deficit, with a size that range from 6-24 km in diameter. This is the first observation of the variation in the secondary cosmic ray air showers covering 700 km^2 in size. Due to the large size of the TASD detector, we can clearly state that the intensity variations in the single count rates observed move in the same direction as the thunderstorms for tens of minutes at a speed of $\sim$ 20 km/10 minutes. These variations are both seen in correlation with lightning (using NLDN) and thunderstorms (using radar images) in the absence of lightning.

To interpret the effect of the electric field inside thunderstorms on the variation of the cosmic ray secondary shower flux, Monte Carlo simulations are performed with CORISKA. First, cosmic rays air showers are propagated in multiple electric field models, then the secondary shower particles (both soft and hard components of the shower) are propagated through the detector following the same trigger condition of the data used in this analysis. The total number of particles is then recorded and

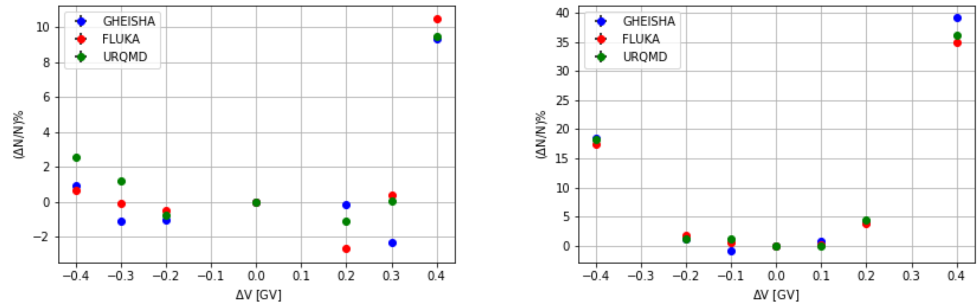

FIG. 5. left: $(\Delta N/N)\%$ vs. ΔV , including statistical error, for a uniform electric field layer inside the cloud (**Intra-Cloud model**) using the three low energy model GHEISHA, FLUKA, and URQMD. The model uses a uniform electric field 2 km inside the thundercloud that is located 2 km above ground level. right: $(\Delta N/N)\%$ vs ΔV, including statistical error, for a uniform electric field layer between the cloud and ground (**Cloud-to-Ground model**) using the three low energy model GHEISHA, FLUKA, and URQMD. In this model the thundercloud base is 2 km in height from the detector .

compared to simulation sets with no electric field. This simplified models used reproduced both the excess and deficit observed in the variation in the cosmic ray air shower flux. The electric field magnitude found to reproduce the observed intensity variations was approximately between 0.2-0.4 GV, depending on the electric field model used and the direction of the electric field. Compared to previous observations, the potential difference recorded by TASD is larger than the reported maximum potential in balloon sounding (0.13 GV) [12]. However, the largest potential difference observed by a cosmic ray detector, thus far, was reported by the Grapes-3 Muon Telescope, with a potential difference of 1 GV [11].

In order to interpret the observations of $\Delta N/N$ by the TASD, more precisely, it is clear that we need to know the polarity of the thunderstorm. This could in principle be achieved by implementing an array of Electric Field Mills (EFMs) at the Telescope Array site. This will allow us to better understand the polarity of the observed thunderstorms and therefore model them. Currently, an Electric Field Mill remote station has been installed approximately in the middle of the Telescope Array site for testing. This will enable us to study the relation between SD observations and the development of thunderstorm's electric field as it progresses on top of the Telescope Array detector.

VII. ACKNOWLEDGEMENTS

Operation and analyses of this study have been supported by NSF grants AGS-1844306 and AGS-2112709. The Telescope Array experiment is supported by the Japan Society for the Promotion of Science(JSPS) through Grants-in-Aid for Priority Area 431, for Specially Promoted Research JP21000002, for Scientific Research (S) JP19104006, for Specially Promoted Research JP15H05693, for Scientific Research (S) JP15H05741, for Science Research (A) JP18H03705, for Young Scientists (A) JPH26707011, and for Fostering Joint International Research (B) JP19KK0074, by the joint research program of the Institute for Cosmic Ray Research (ICRR), The University of Tokyo; by the U.S. National Science Foundation awards PHY-0601915, PHY-1404495, PHY-1404502, and PHY-1607727; by the National Research Foundation of Korea (2016R1A2B4014967, 2016R1A5A1013277, 2017K1A4A3015188, 2017R1A2A1A05071429) ; by the Russian Academy of Sciences, RFBR grant 20-02-00625a (INR), IISN project No. 4.4502.13, and Belgian Science Policy under IUAP VII/37 (ULB). The foundations of Dr. Ezekiel R. and Edna Wattis Dumke, Willard L. Eccles, and George S. and Dolores Doré Eccles all helped with generous donations. The State of Utah supported the project through its Economic Development Board, and the University of Utah through the Office of the Vice President for Research. The experimental site became available through the cooperation of the Utah School and Institutional Trust Lands Administration (SITLA), U.S. Bureau of Land Management (BLM), and the U.S. Air Force. We appreciate the assistance of the State of Utah and Fillmore offices of the BLM in crafting the Plan of Development for the site. Patrick Shea assisted the collaboration with valuable advice on a variety of topics. The people and the officials of Millard County, Utah have been a source of steadfast and warm support for our work which we greatly appreciate. We are indebted to the Millard County Road Department for their efforts to maintain and clear the roads which get us to our sites. We gratefully acknowledge the contribution from the technical staffs of our home institutions. An allocation of computer time from the Center for High Performance Computing at the University of Utah is gratefully acknowledged. We thank Ryan Said and W. A. Brooks of Vaisala Inc. for providing quality NLDN data lightning discharges over and around the TASD under their academic research use policy.

[1] M. Stolzenburg *et al.*, "Electric field values observed near lightning flash initiations," *Geophysical Research Letters*, vol. 34, no. 4, 2007.

[2] W. P. Winn and other, "Measurements of electric fields in thunderclouds," *Journal of Geophysical Research (1896-1977)*, vol. 79, no. 12, pp. 1761–1767, 1974.

[3] V. V. Alexeenko *et al.*, "Short Perturbations of Cosmic Ray Intensity and Electric Field in Atmosphere," in *International Cosmic Ray Conference*, vol. 4 of *International Cosmic Ray Conference*, p. 272, Jan. 1987.

[4] Eastop Collaboration, "The EAS counting rate during thunderstorms," in *International Cosmic Ray Conference*, vol. 10 of *International Cosmic Ray Conference*, p. 4165, Aug. 2001.

[5] H. Tsuchiya *et al.*, "Observation of thundercloud-related gamma rays and neutrons in Tibet," *Phys. Rev. D*, vol. 85, p. 092006, May 2012.

[6] B. Bartoli *et al.*, "Observation of the thunderstorm-related ground cosmic ray flux variations by ARGO-YBJ," *Phys. Rev. D*, vol. 97, no. 4, p. 042001, 2018.

[7] K. Kudela *et al.*, "Correlations between secondary cosmic ray rates and strong electric fields at lomnick tt," *Journal of Geophysical Research: Atmospheres*, vol. 122, no. 20, pp. 10,700–10,710, 2017.

[8] H. Tsuchiya *et al.*, "Long-duration gamma ray emissions from 2007 and 2008 winter thunderstorms," *Journal of Geophysical Research: Atmospheres*, vol. 116, no. D9, 2011.

[9] Y. Muraki *et al.*, "Effects of atmospheric electric fields on cosmic rays," *Phys. Rev. D*, vol. 69, p. 123010, Jun 2004.

[10] C.T.R. Wilson in *Proc. R. Soc. Lond. A*, vol. 236, p. 297, 1956.

[11] B. Hariharan *et al.*, "Measurement of the electrical properties of a thundercloud through muon imaging by the GRAPES-3 experiment," *Phys. Rev. Lett.*, vol. 122, p. 105101, Mar 2019.

[12] T. C. Marshall and M. Stolzenburg, "Voltages inside and just above thunderstorms," *Journal of Geophysical Research: Atmospheres*, vol. 106, no. D5, pp. 4757–4768, 2001.

[13] T. Abu-Zayyad *et al.*, "The surface detector array of the Telescope Array experiment," *Nuclear Instruments and Methods in Physics Research A*, vol. 689, pp. 87–97, Oct. 2012.

[14] R. U. Abbasi *et al.*, "Gamma ray showers observed at ground level in coincidence with downward lightning leaders," *Journal of Geophysical Research: Atmospheres*, vol. 123, no. 13, pp. 6864–6879, 2018.

[15] D. Heck *et al. Report FZKA 6019*, vol. Forschungszentrum Karlsruhe, 1998.

[16] E.-J. Ahn, R. Engel, T. K. Gaisser, P. Lipari, and T. Stanev, "Cosmic ray interaction event generator SIBYLL2.1," *Phys. Rev. D*, vol. 80, p. 094003, Nov 2009.

[17] H. Fesefeldt *Report PITHA-85/02*, vol. RWTH Aachen, 1985.

[18] S. Bass *et al.*, "Microscopic models for ultrarelativistic heavy ion collisions," *Progress in Particle and Nuclear Physics*, vol. 41, pp. 255–369, 1998.

[19] A. Fasso *et al.*, "The Physics models of FLUKA: Status and recent developments," *eConf*, vol. C0303241, p. MOMT005, 2003.

VIII. SUPPLEMENTAL MATERIAL

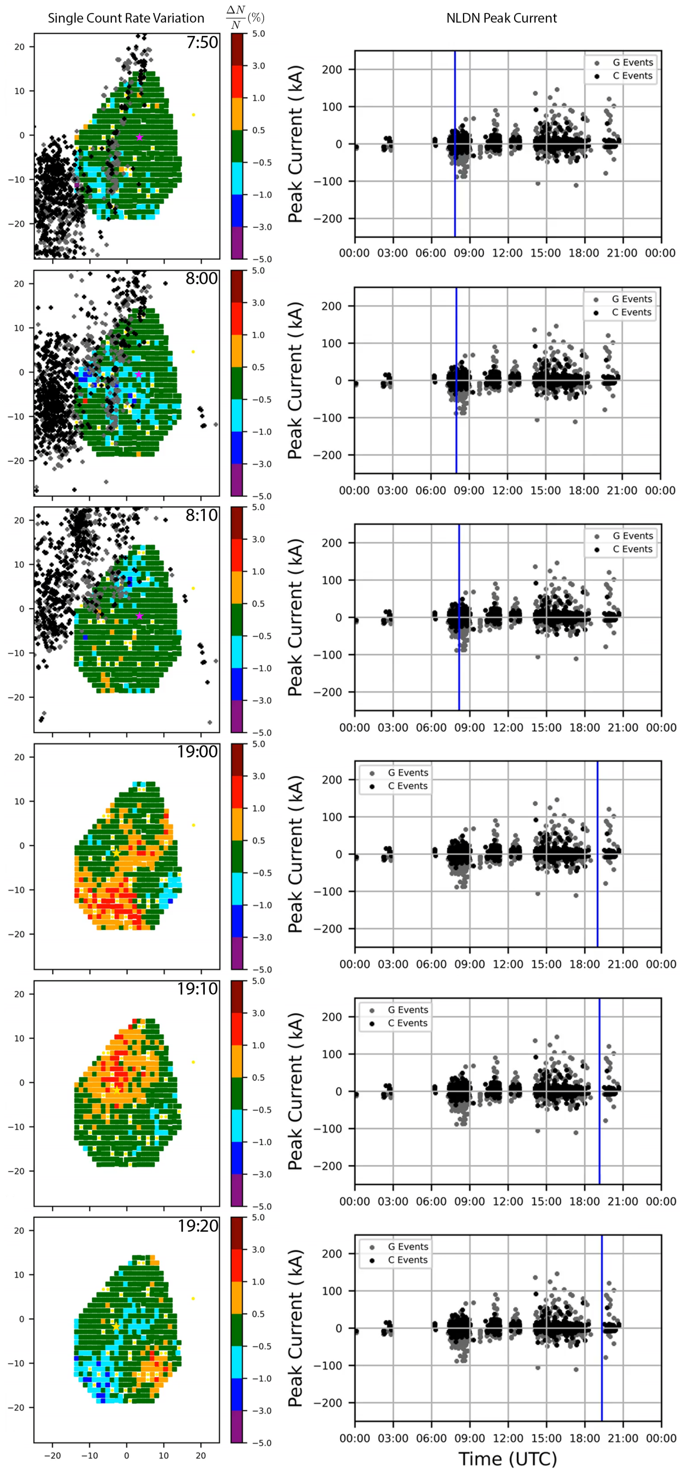

FIG. 6. **Supporting Information 1 (SI1):** left: Time evolution of the intensity variation of the secondary low-energy cosmic-ray counting rate change ($\frac{N_c - N_p}{N_p}$) or ($\Delta N/N$) on the 09/27/2014 thunderstorm shown in Figure 2. Right: NLDN events peak current (kA) vs. time of the day in UTC. The blue line denotes the starting time for each frame on the left hand side. The black and grey cross marks are the Intra-Cloud and Cloud-to-Ground lightning sources detected by the NLDN for each frame.

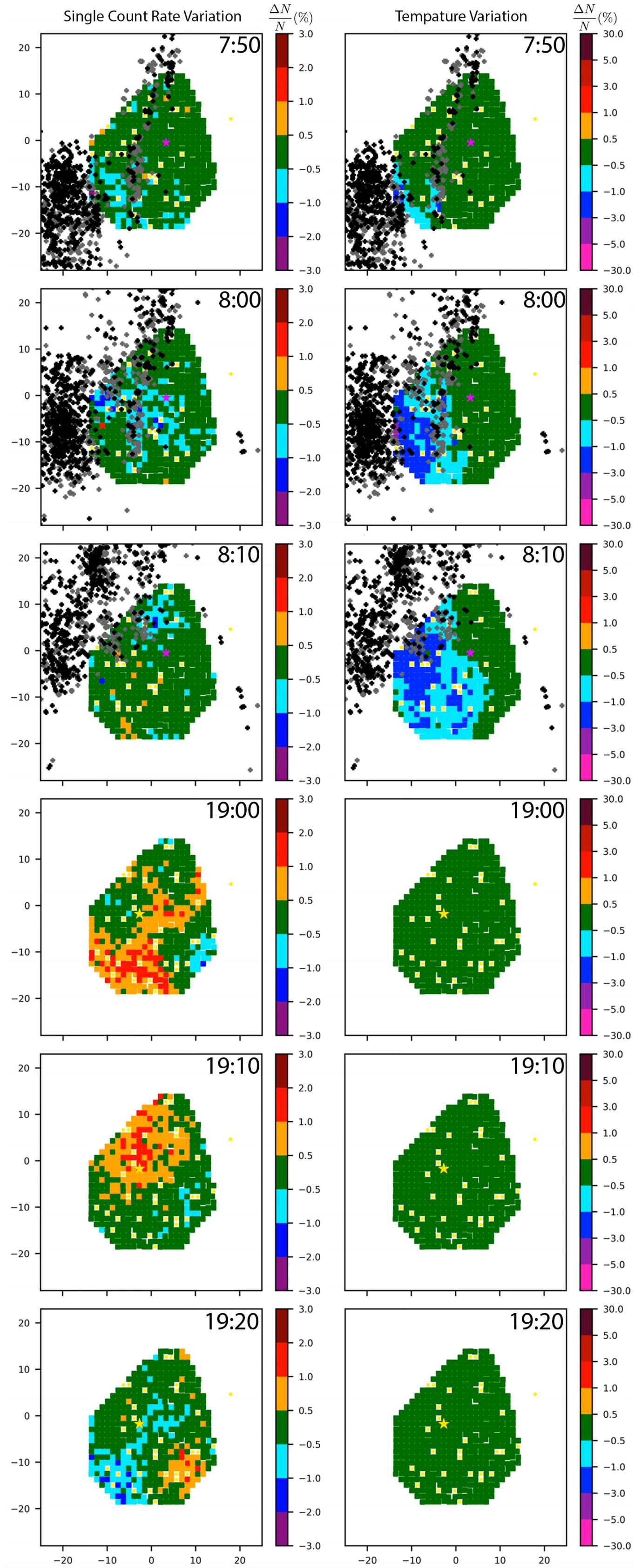

FIG. 7. **Supporting Information 2 (SI2):** left: Time evolution of the intensity variation of the secondary low-energy cosmic-ray counting rate change ($\frac{N_c - N_p}{N_p}$) or ($\Delta N/N$) on the 09/27/2014 thunderstorm shown in Figure 2. Right: Temperature variation at 1400 m ($T_c - T_p$) or (ΔT) for the same frames. T_c is the temperature in the current frame and T_p is the temperature in the previous frame. The starting time is denoted on each frame. The black and grey crosses marks are the Intra-Cloud and Cloud-to-Ground lightning sources detected by the NLDN for each frame.

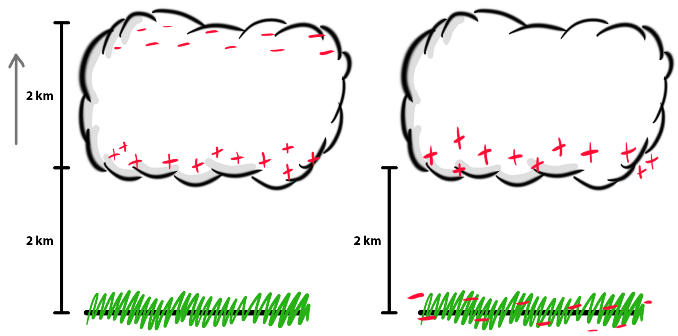

FIG. 8. **Supporting Information 3 (SI3):** An illustration of the models used in the simulation in this work is to quantify the electric field inside thunderstorms resulting in the observed variations in the EAS by the TASD detector. left: The model using a uniform electric field 2 km inside the thundercloud (**Intra-Cloud model**) that is located 2 km above ground level. right: The model using a uniform electric field 2 km above ground level (**Cloud-to-Ground model**). The grey arrow represents the direction of the positive electric field following CORSIKAs definition, where positive electric field direction is pointing upwards.

Supporting Information 4 (SI4): https://youtu.be/608Jm8dujHc. Time evolution of the radar images for the 09/27/2014 thunderstorm from 06:25 - 08:55 including the Telescope Array location marked in red. The image was extracted from https://www2.mmm.ucar.edu/imagearchive/image

Supporting Information 5 (SI5): https://youtu.be/V7yIh9wmM30. Time evolution of the radar images for the 09/27/2014 thunderstorm from 18:25 - 19:50 including the Telescope Array location marked in red. The image was extracted from https://www2.mmm.ucar.edu/imagearchive/image

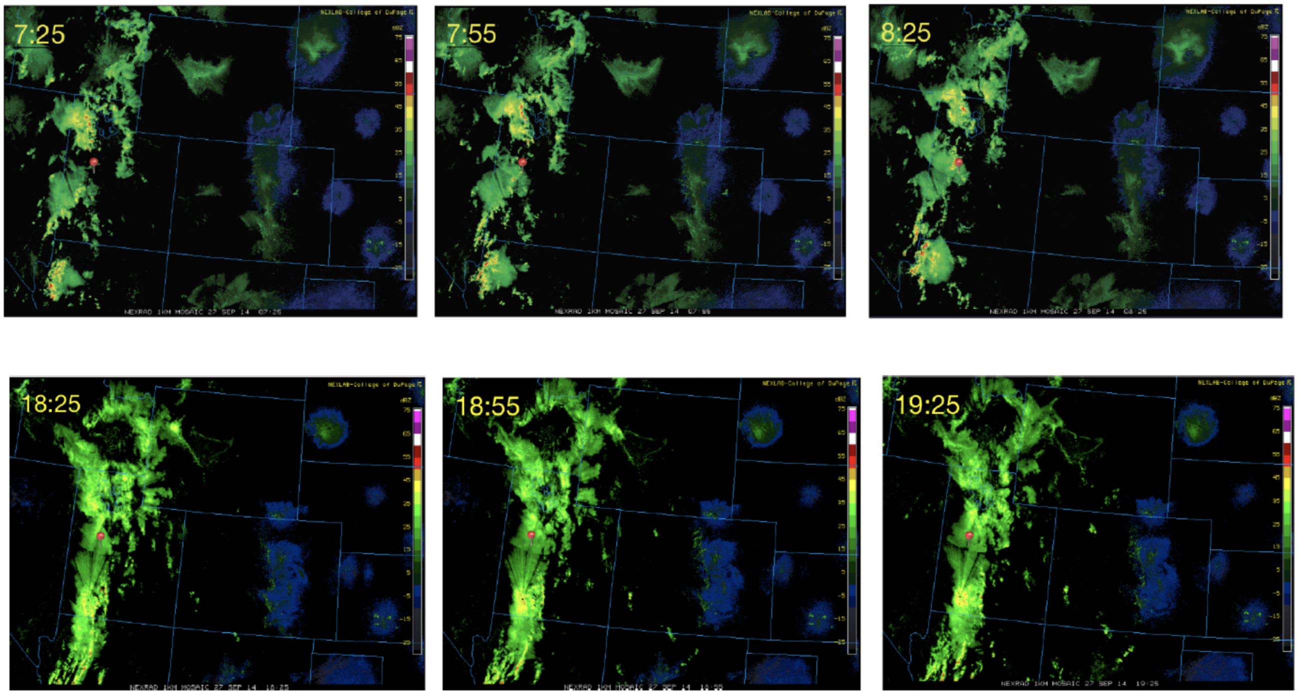

FIG. 9. **Supporting Information 6 (SI6):**Top: Time evolution of the intensity variation of the radar images for the 09/27/2014 thunderstorm from 07:25 - 08:55 including the Telescope Array location marked in red. Bottom: Time evolution of the intensity variation of the radar images for the 09/27/2014 thunderstorm from 18:25 - 19:55 including the Telescope Array location marked in red.